Phase Behavior of Isotactic Polypropylene−Poly(ethylene/ethylethylene) Random Copolymer Blends

Peter A. Weimann, Todd D. Jones, Marc A. Hillmyer, and Frank S. Bates*

Department of Chemical Engineering and Materials Science, University of Minnesota, Minneapolis, Minnesota 55455

J. D. Londono, Yuri Melnichenko, and George D. Wignall

Oak Ridge National Laboratory, Oak Ridge, Tennessee 37831-6393

Kristoffer Almdal

Risø National Laboratory, DK-4000 Roskilde, Denmark

Received September 17, 1996; Revised Manuscript Received March 7, 1997⊗

ABSTRACT: The melt-state phase behavior of isotactic polypropylene (i-PP) blended with a series of poly(ethylene/ethylethylene) random copolymers has been investigated using small-angle neutron scattering (SANS). These PEE*xx* copolymers, where *xx* is the percentage of ethylethylene (EE) units, were prepared by hydrogenation of anionically polymerized polybutadienes with controlled amounts of 1,2 addition. Random phase approximation (RPA) fits to the scattering data for blends of i-PP with a deuterated, low molecular weight PEE90 at 180 °C indicate a statistical segment length for i-PP that is 10% less than that reported previously. Scattering from blends of i-PP with higher molecular weight PEE90 and PEE73 at 180 °C can be quantitatively fit using the RPA theory with χ as the only adjustable parameter, indicating melt miscibility. PEE46 and PEE62 are strongly and marginally immiscible, respectively, with i-PP at 180 °C. These results establish a "window" in EE content in which these random copolymers can form single phase mixtures with i-PP.

1. Introduction

Isotactic polypropylene (i-PP) is a saturated hydrocarbon polymer governed by nonspecific dispersive interactions, leading to nearly athermal mixing with other saturated hydrocarbons. Nevertheless, it is well-known that i-PP phase separates from most other polyolefins, including polyethylene,[1−3] poly(ethylenepropylene) rubber (EPR),[4−6] and polyisobutylene.[7] Recently, we have performed studies focused on gaining a better understanding of experimental and theoretical aspects of polyolefin thermodynamics, with an emphasis on mixtures that contain commercial i-PP.[8,9] In this paper, we describe experiments confirming the melt miscibility of i-PP with poly(ethylene/ethylethylene) random copolymers, denoted PEE*xx*, where *xx* refers to the percentage of hydrogenated 1,2 additions in a saturated 1,4/1,2-polybutadiene random copolymer. The microstructures of i-PP and PEE*xx* polymers are shown in Figure 1.

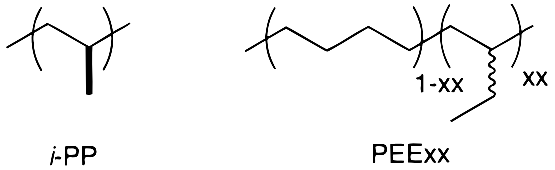

Figure 1. Microstructures of i-PP and PEE*xx* polymers.

Nonideal mixing in polyolefin blends has been the subject of much attention in recent years. Two ambitious theoretical approaches to the larger problem of polymer−polymer thermodynamics are the polymer reference interaction site model (PRISM) of Schweizer and co-workers[10−14] and the lattice cluster theory of Dudowicz and Freed.[15,16] Although both of these first-principles theories are relevant to our work, a quantitative assessment of them would be well beyond our present scope.

The semiempirical solubility parameter formalism adopted by Graessley and co-workers in evaluating their experimental results on polyolefin blends[17−25] provides a tractable alternative for dealing with such mixtures. This treatment, based on regular solution theory, assumes that the Flory−Huggins interaction parameter (χ) of a blend is described by the difference in the solubility parameters (δ) of the two components. If unique solubility parameters can be assigned to each component of a new polyolefin mixture, phase behavior may be predicted. Solubility parameters have been determined for a series of amorphous saturated hydrocarbon polymers, either through direct measurement of χ by small-angle neutron scattering (SANS)[22−24] or through determination of *PVT* properties.[23] Notably, i-PP has not been included in the matrix of saturated hydrocarbon polymers studied by Graessley et al.[22−24]

This extensive body of experimental work has revealed several interesting nonideal mixing effects in polyolefin blends yet to be accounted for by present theories of polyolefin phase behavior. One is the "deuterium swap" effect[19,20] in which the magnitude of χ, as measured by SANS, depends upon which component of the blend is labeled with deuterium, a phenomenon also noted by others.[26,27] In blends of saturated polybutadienes of varying branch contents, these studies have all found that labeling of the component with higher branch content tends to increase χ. "Irregular mixing" has also been observed in some polyolefin blends,[24] for which the reported χ parameter varied from that calculated on the basis of the solubility parameters of the individual components. About 25% of the mixtures in these studies fall into the "nonideal" category.[24] Observation of the "deuterium swap" effect and the nonuniversal variations in the temperature dependence of χ in their blends led Graessley et al. to comment that

---

[*] To whom correspondence should be addressed.

[⊗] Abstract published in *Advance ACS Abstracts,* May 15, 1997.

S0024-9297(96)01383-6 CCC: $14.00

the "interactions between saturated hydrocarbons are primarily enthalpic."[24]

The conformational asymmetry theory developed by Fredrickson et al.[28−30] is an alternative approach to the description of nonideal mixing in polyolefin blends. In this treatment, a correlation is established between differences in statistical segment length and the excess free energy of mixing. The statistical segment length (b) is related to the radius of gyration (R_g) of a polymer by

$$R_g = b(N/6)^{1/2} \tag{1}$$

where N is the number of statistical segments. On the basis of data from polyolefin blends and block copolymers, Bates et al.[31] reported a correlation between the magnitude of χ and the asymmetry in the statistical segment lengths of the two components or blocks, a result also observed by Graessley et al.[24] Bates et al.[31] speculated that the excess free energy of mixing in these blends might result from an entropic penalty associated with nonlocal conformational rearrangements that accompany mixing.

A theoretical treatment of this hypothesis has been developed using a parameter β (originally defined by Helfand and Sapse[32]) that describes the conformation of a polymer independent of its degree of polymerization,

$$\beta_i^2 = \frac{b_i^2}{6v_i} \tag{2}$$

The excess interaction energy density α_ϵ for an athermal blend of homopolymers A and B is related to the second derivative of the excess free energy density F^E with respect to component volume fraction ϕ_A,[30]

$$\alpha_\epsilon \equiv \frac{1}{2k_BT}\frac{\partial^2 F^E}{\partial \phi_A^2} = \frac{\Lambda_b^3}{24\pi^2}\left[\frac{1-\epsilon}{\phi+(1-\phi)\epsilon}\right]^2 \tag{3}$$

$$\epsilon = \left(\frac{\beta_A}{\beta_B}\right)^2 \tag{4}$$

where Λ_b^{-1} is a cutoff length that separates local (segmental-scale) and nonlocal mixing effects[30] and ϵ is a dimensionless parameter describing the degree of conformational symmetry. α_ϵ may be related to the $\tilde{\chi}$ parameter measured using small angle scattering by[30]

$$\tilde{\chi}_\epsilon = \alpha_\epsilon (v_A v_B)^{1/2} \tag{5}$$

where $\tilde{\chi} = \tilde{\chi}_\epsilon$ in the limit of athermal mixing. Ideal mixing is recovered for the conformationally symmetric case ($\epsilon = 1$). Graessley et al.[24] have noted that estimates of Λ_b^{-1} based on $\tilde{\chi}$ parameters measured for model polyolefin blends indicate that $\Lambda_b^{-1} \approx 0.25\ (b_A b_B)^{1/2}$, which is inconsistent with the nonlocal nature of the theory.

Extensive experimental work has been performed on i-PP blends during the last four decades. We briefly review some of the more recent work pertaining to the phase behavior of blends of i-PP with other saturated polyolefins; a review of much of the older literature in this field was provided by Plochocki.[1] The immiscibility of melt-blended HDPE and i-PP in the crystalline state has been reported on the basis of results from optical and electron microscopy.[2] PE/i-PP phase separation has also been observed in the melt using SANS.[3] Optical microscopy has been used to show that crystallized polyisobutylene/i-PP blends exhibit a two-phase structure.[7] Phase-separated structures have also been documented[4−6] for blends of i-PP with several EPR samples of varying propylene contents. Most notably, Lohse[6] has used SANS to measure melt phase separation in several i-PP/EPR blends, including a blend of i-PP with a 91.6 wt % propylene EPR. Significantly, the only sample in this study that was found to be melt-miscible with i-PP at 200 °C was a polydisperse atactic polypropylene, with $M_w/M_n = 14.79$.[6]

Prior to our work, isotactic poly(1-butene)[33] (i-P1B) has been the polymer most often identified as being compatible with i-PP, although there have been conflicting reports of the miscibility of these materials. Amorphous-state miscibility across the full range of compositions has been claimed on the basis of the observation of one glass transition temperature in a series of blends[34] and reductions in the equilibrium melting temperature of the i-PP component in blends.[35] In contrast, another report claimed miscibility of i-PP/i-P1B blends occurs only for i-PP concentrations below 20% or above 80%.[36] Cham et al.[37] have directly observed liquid−liquid phase separation in an i-PP/i-P1B 70/30 (w/w) blend by optical microscopy and noted growth of i-PP spherulites in both coexisting liquid phases above the melting point of i-P1B. These features, coupled with an observation of a single glass transition by dynamic mechanical analysis, led Cham et al.[37] to suggest "a significant degree of molecular-level mixing in each phase." In addition, Bartczak et al.[38] have reported that i-PP/i-P1B blends quenched immediately after melt blending show a homogeneous morphology, while samples allowed to anneal display a phase-separated structure. Taken together, the body of work in this area suggests that these two polymers are partially miscible, with phase-separation kinetics often controlling the observed microstructure.

A different approach to the exploration of the thermodynamics of i-PP blends has been taken by our group.[8,9] Previous experimental work[31] and the conformational asymmetry theory[30] described by eqs 3 and 4 both suggest that the excess free energy of mixing of a polyolefin blend will be minimized when $\epsilon = 1$. Guided by these results, we developed model polyolefins in homopolymer and block copolymer architectures that are compatible with i-PP. Using the SANS data of Ballard et al.,[39] we calculated $\beta_{\text{i-PP}}^2 \approx 5.2 \times 10^{-2}$ Å^{-1} at 175 °C. On the basis of measurements of β for PE and PEE, we concluded that i-PP would be conformationally symmetric with PEE73, an amorphous, atactic statistical copolymer of ethylene and ethylethylene (EE) with 73% EE repeat units.[8] Using sequential anionic polymerization followed by catalytic hydrogenation, we prepared a polystyrene−PEE73 diblock copolymer that was completely melt-dispersible in i-PP,[8] suggesting that i-PP and PEE73 are thermodynamically compatible. Here, we report a SANS study of the melt phase behavior of blends of i-PP with a series of hydrogenated polybutadiene homopolymers of varying branch contents. An important component of this study is a new measurement of the statistical segment length of i-PP using a deuterated, low molecular weight PEE90 polymer as a "polymeric solvent". This investigation quantitatively establishes the melt miscibility of PEE*xx* random copolymers with i-PP over a restricted range of ethylethylene content, confirming our prior speculation.[8]

Table 1. General Butadiene Polymerization Conditions

polybutadiene microstructure: % 1,2 addition	[THF]:[Li][a]	temp, °C	time, h
46 ± 1	45:1	40	18
62 ± 1	85:1	30	24
73 ± 1	85:1	20	36
90 ± 1	pure THF	−55	8−24

[a] In cyclohexane.

2. Experimental Section

Materials. Cyclohexane used in polymerizations was purified by distillation from an orange poly(styryllithium) solution, while THF used in polymerizations was purified by distillation from purple Na/benzophenone solution, both under argon. Butadiene (Aldrich) was purified by successive distillation from dibutylmagnesium (Aldrich) and *n*-butyllithium (Aldrich). 1,1,4,4-Tetradeuteriobutadiene was prepared from butadienyl-2,2,5,5-d_4 sulfone (Aldrich) using procedures described elsewhere[40] and purified in the same manner as perprotiobutadiene. *sec*-Butyllithium (Aldrich) was used as received, and the concentration of active anion in this initiator was measured using the double titration technique of Gilman and Cartledge.[41] $Pd/CaCO_3$ (5%, Strem) was used as received for heterogeneous catalytic hydrogenation. Cyclohexane for hydrogenation reactions was sparged with argon before use. Deuterous and hydrogenous chloroform, methanol, 2-propanol, ethylene glycol, decahydronaphthalene, and THF for size exclusion chromatography (SEC) were all used as received. Isotactic polypropylene (Escorene PP3045, a nonwoven fiber grade resin with a melt flow rate of 37 g/10 min) was generously supplied by Exxon Chemical Co. This material, referred to as PP3045, was used as received.

Anionic Polymerization. Five hydrogenous polybutadiene polymers, with 46, 62, 73, and 90% 1,2 addition, were synthesized using documented anionic polymerization techniques.[40,42] A mixture of cyclohexane and THF was used for synthesis of the 46, 62, and 73% 1,2-polybutadienes, with the amount of 1,2 addition controlled by the [THF]:[Li] ratio.[43] Pure THF was used as the solvent for the preparation of the 90% 1,2-polybutadienes. The conditions for each reaction are given in Table 1. In each case, the amount of 1,2 addition was verified using solution ^1H NMR spectroscopy (Varian VXR-500) at 20 °C, through comparison of the integrated area of the characteristic vinyl (1,2) and olefin (1,4) resonances[44] occurring between 4.8 and 6.0 ppm. A pulse delay time of 30 s was employed to ensure complete relaxation, leading to an estimated error of ±1% in the reported 1,2 content.

The polydispersity of each reaction product was determined by size exclusion chromatography (SEC) (Altex differential pump, Rheodyne injector, 4 Phenomenex phenogel columns with 5×10^5, 5×10^4, 5×10^3, and 500 Å pore sizes, and a Waters R401 differential refractometer), with THF or chloroform as the mobile phase. All samples had a polydispersity (N_w/N_n) of less than or equal to 1.07, based on comparison with polystyrene standards.

A low molecular weight, partially deuterated polybutadiene (d_4PB90) was produced by polymerization of 1,1,4,4-tetradeuteriobutadiene in THF. The number-average degree of polymerization (N_n) of this polymer was determined by end-group analysis of the ^1H NMR spectrum taken at 20 °C,[40] assuming 90% 1,2 addition. Through comparison of the integrated peak area of the proton resonances of the *sec*-butyl initiator fragment at approximately 0.85 ppm to the integrated area of the olefin peaks occurring between 5.2 and 5.7 ppm, we obtained $N_n = 171 \pm 9$ for this polymer. SEC analysis of this material yielded $N_w/N_n = 1.03$. A fully hydrogenous polybutadiene (PB90C) was prepared under the same conditions, with $N_n = 236 \pm 12$ and $N_w/N_n = 1.04$.

Catalytic Saturation. All polybutadienes were saturated through reaction with either H_2 or D_2 at 500 psi and 70 °C over the 5% $Pd/CaCO_3$ catalyst for approximately 16 h. Polymer concentrations in cyclohexane ranged from 10 to 30 g/L, and the amount of catalyst varied between 2 and 3 times the weight of the polymer. Reactions were performed in either a Parr Instrument Co. high-pressure reactor or a specially designed pressure reactor.[45] In all cases, saturation was confirmed by the disappearance of the characteristic vinyl and olefin resonances between 4.8 and 6.0 ppm in the ^1H NMR spectrum. The saturated polymers are referred to as PEE*xx*, where *xx* is the percentage of 1,2 addition in the butadiene precursor.[46] These copolymers are derived from random 1,4/1,2-butadiene copolymers, and the resulting compounds are random copolymers of ethylene and ethylethylene. The polyethylene segments consist of four main-chain $-(CH_2)-$ units, as illustrated in Figure 1.

Matched pair hydrogenated and partially deuterated samples were prepared for each PEE*xx* polymer; the latter are referred to as PEE*xx*d. The degree of polymerization for each of these materials was measured by SANS experiments performed on matched-pair, $\phi_d = 0.5$ blends (discussed below), with the exception of the PEE90A sample, for which the degree of polymerization was taken from the anionic polymerization reaction stoichiometry. The d_4PB90 specimen was saturated with deuterium and is referred to as d_6PEE90.

Density Measurement. Densities of the PEE*xx* samples were measured by the density gradient column technique, using 2-propanol/ethylene glycol as the medium at 26 °C.[45] The average number of deuterium atoms per repeat unit in the partially deuterated samples (Table 2) is calculated on the basis of these results. Since the density is increasingly sensitive to the changes in molecular weight in the low M_n limit, we prepared the PEE90C material to establish the density of a hypothetical fully hydrogenous $N_n = 171$ sample, for comparison with the d_6PEE90 specimen. Assuming that the density can be described by $\rho^{-1} = x + y/N_n$,[47] and with the measured values for PEE90B and PEE90C, we estimate the density of fully hydrogenous, $N_n = 171$ PEE90 as 0.859 ± 0.002 g/cm^3. Based on this value, we estimate 6.30 ± 0.13 deuterons per d_6PEE90 repeat unit.

Sample Preparation. Isotopic matched pair blends of PEE*xx*h and PEE*xx*d polymers, referred to as PEE*xx*h+d, with a deuterated polymer volume fraction (ϕ_{PEExxd}) of 0.5, were prepared by solvent evaporation from *n*-pentane in air with subsequent drying in vacuum at 60 °C. Matched pair blends were loaded between quartz disks separated by 1.25 mm aluminum spacers and then sealed with adhesive (5-min epoxy, silicone, or Varian Torr-Seal) in an argon-atmosphere glovebox. Blends of PP3045 with PEE46d, PEE62d, PEE73d, and PEE90Ad, also with $\phi_{PEExxd} = 0.5$, were prepared by codissolving the components in decahydronapthalene at 180

Table 2. Polymer Molecular Characteristics

polymer	ρ_H, g cm^{-3} [a]	ρ_D, g cm^{-3} [a]	n_D[b]	N_w	b(25 °C), Å[c]	b(180 °C), Å[f]
PEE46	0.8570 ± 0.0003	0.8935 ± 0.0002	2.32 ± 0.02	1180 ± 60[c]	7.7 ± 0.4	7.4
PEE62	0.8607 ± 0.0002	0.8971 ± 0.0002	2.27 ± 0.02	1470 ± 80[c]	6.5 ± 0.3	6.4
PEE73	0.8650 ± 0.0002	0.8979 ± 0.0002	2.07 ± 0.02	1290 ± 70[c]	6.1 ± 0.3	6.1
PEE90A		0.9086 ± 0.0002	2.50 ± 0.02	630 ± 30[d]		5.2
PEE90B	0.8688 ± 0.0002	0.9068 ± 0.0002	2.38 ± 0.02	1470 ± 80	5.1 ± 0.2	5.2
PEE90C	0.8590 ± 0.0006			236 ± 12[e]		
d_6PEE90		0.9570 ± 0.0003	6.30 ± 0.13	171 ± 9[e]		5.2
PP3045				1260 ± 170[c]		5.6 ± 0.2[c]

[a] All densities measured at 26 °C. ρ_H and ρ_D refer to the polymer saturated with hydrogen and deuterium, respectively. [b] Average number of deuterons per C_4 repeat unit. [c] Determined by SANS. [d] Based on reaction stoichiometry and SEC. [e] Based on ^1H NMR and SEC. [f] Estimated from b(25 °C) and $(\partial \ln R_g/\partial T)$.[57,58]

°C, followed by precipitation in cold methanol. The precipitate was dried in air, followed by further drying for 12 h at 100 °C under vacuum. Blends were then loaded within aluminum spacers mounted on quartz disks, and allowed to flow into the neutron cells by heating under vacuum for 6 h at approximately 200 °C.[48] After cooling, these samples were sealed under argon. Two d_6PEE90/PP3045 blends, with $\phi_{PP3045} = 0.124$ and 0.173, were prepared by loading appropriate amounts of the neat polymers and a small stir bar in a 1.02 mm thick cylindrical quartz cell. The cell openings were then sealed with epoxy under flowing argon. The mixtures were homogenized by stirring on a hot plate at approximately 220 °C for at least 2 h, followed by rapid cooling, which induced crystallization.[48]

Small Angle Neutron Scattering. The majority of the SANS measurements reported here were performed using the W. C. Koehler 30 m SANS instrument at Oak Ridge National Laboratory, Oak Ridge, TN. Experiments were conducted with a neutron wavelength $\lambda = 4.75$ Å ($\Delta\lambda/\lambda = 0.06$) and a sample-to-detector distance of 10 m. Raw data were corrected for detector sensitivity and beam-blocked instrumental backgrounds and normalized to sample transmission and sample thickness. Absolute intensity calibration was accomplished using Al-4 aluminum and Porasil B secondary standards, as described elsewhere.[49] All scattering patterns were azimuthally averaged to produce one-dimensional plots of absolute intensity versus the magnitude of the scattering wavevector $q = (4\pi/\lambda)\sin(\theta/2)$, where θ is the scattering angle. Additional measurements were made using the NIST/Exxon/University of Minnesota 30 m SANS instrument at the National Institute of Standards and Technology, Gaithersburg, MD ($\lambda = 7.0$ Å, $\Delta\lambda/\lambda = 0.09$, sample-to-detector distance of 10 m), and the 12 m SANS instrument located at the Risø National Laboratory, Roskilde, Denmark ($\lambda = 5.6$ Å, $\Delta\lambda/\lambda = 0.09$, sample-to-detector distance of 5 m). Similar data reduction and analysis procedures were used with these instruments.

SANS measurements of PEE*xx*h+d mixtures were conducted at room temperature, while the i-PP containing samples were examined at 180 °C. The d_6PEE90/PP3045 specimens were thermally equilibrated prior to acquisition of SANS data, through heating for approximately 30 min at 205 °C, followed by annealing for approximately 20 min at 180 °C in the sample stage. PEE*xx*/PP3045 samples were equilibrated by heating for 15 min at 220 °C, followed by an additional 15 min of annealing at 180 °C in the sample stage. In conjunction with the sample preparation technique, this procedure provides adequate time for single-phase mixtures to homogenize, while permitting phase separation to occur in thermodynamically incompatible blends.

We observed excess scattering intensity at $q < 0.09$ nm^{-1} in data taken from some of the undiluted PEE*xx* blank samples, PEE*xx*h+d blends, and PEE*xx*/PP3045 blends. As noted in a previous publication,[50] we believe this scattering is due to residual hydrogenation catalyst in the saturated PEE*xx* materials.[51] To ensure that this effect did not interfere with quantitative analysis of the data, we have discarded all data below $q = 0.09$ nm^{-1}.

3. Results and Analysis

Background Corrections. Plots of the total scattered intensity as a function of q for undiluted PEE46d, PEE62d, PEE73d, PEE90Ad, and PEE73h are shown in Figure 2. All of the fully hydrogenous samples produced essentially q-independent profiles above $q = 0.09$ nm^{-1}, consistent with primarily incoherent scattering, as illustrated by the data from PEE73h. Three of the partially deuterated compounds (PEE46d, PEE62d, PEE73d) exhibited a significant forward scattering component. This effect has been attributed to nonuniform labeling of individual chains in the heterogeneous catalytic deuteration reaction.[52,53] Balsara et al.[52] have shown that forward scattering from such samples has both coherent and incoherent components. They assumed that the high-q asymptote of the scattering pattern can be taken as the incoherent level for the sample. After subtraction of this incoherent component from the scattering data, it was found[52] that the residual coherent intensity could be fit to the function

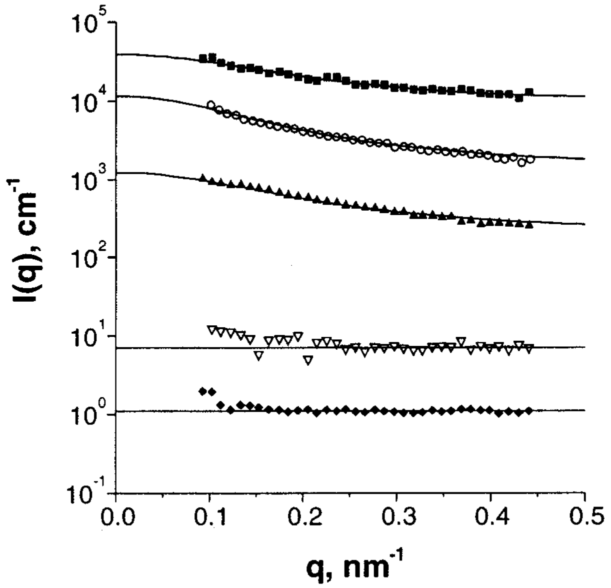

Figure 2. Total SANS intensity for undiluted PEE46d (filled triangles), PEE62d (open circles), PEE73d (filled squares), PEE90Ad (open triangles), and PEE73h (filled diamonds). Data sets have been progressively offset by a factor of 10. For clarity, only 50% of the actual data points are shown. The solid curves through the 46d, 62d, and 73d scattering patterns represent best fits to eqs 6−8 plus a constant corresponding to the incoherent, high-q asymptote. The 90Ad and 73h patterns are shown with flat lines corresponding to the value calculated for incoherent scattering from these samples.

$$I'_c(q) = (\overline{B^2} - \bar{B}^2)Nvg_D(x) \tag{6}$$

where $\overline{B^2}$ is the average square contrast, $\bar{B}^2$ is the average contrast squared, N is the degree of polymerization, v is the segment volume, and $g_D(x)$ is the Debye function,[54]

$$g_D(x) = (2/x^2)(e^{-x} - 1 + x) \tag{7}$$

where

$$x = q^2{R_g}^2 \tag{8}$$

We have fit the coherent component of the PEE46d, PEE62d, and PEE73d data to eqs 6−8 using a nonlinear least-squares fitting technique, with the prefactor $(\overline{B^2} - \bar{B}^2)Nv$ and R_g as independent variables, as shown in Figure 2. These results are consistent with the explanation of the origin of coherent forward scattering proposed by Balsara et al.[52] and Reichart et al.[53] We have subsequently corrected the data for all blend samples containing PEE46d, PEE62d, or PEE73d by subtracting the estimated incoherent background for each component *and* the coherent background contribution of the partially deuterated material from the total scattering intensity.[52]

Curiously, the SANS profile from the pure PEE90Ad material did not contain a significant coherent component, as shown in Figure 2. We attribute this to variations in heterogeneous catalytic hydrogenation conditions.

PEE*xx* Degree of Polymerization and Statistical Segment Length. Degrees of polymerization and

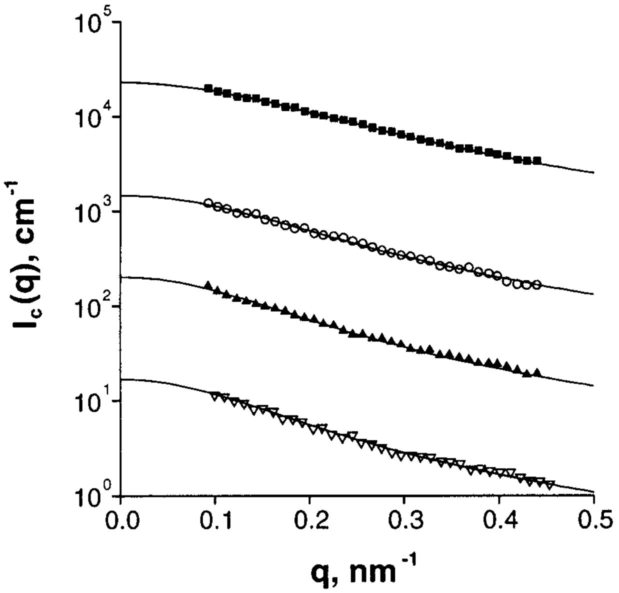

Figure 3. Background-corrected SANS results for $\phi_d = 0.5$ matched pair blends at 25 °C: PEE46h+d (open triangles), PEE62h+d (filled triangles), PEE73h+d (open circles), and PEE90Bh+d (filled squares). Data sets have been progressively offset by a factor of 10. For clarity, only 50% of the actual data points are shown. Solid curves correspond to best fits to eqs 7−10 with the degree of polymerization *N* and statistical segment length *b* as adjustable parameters. Results of these fits are given in Table 2.

statistical segment lengths of PEE46, PEE62, PEE73, and PEE90B were determined by fitting the random phase approximation (RPA) structure factor for a two-component, homogeneous blend of monodisperse polymers,[55]

$$S^{-1}(q) = [\phi_A N_A g_D(x_A)]^{-1} + [(1 - \phi_A) N_B g_D(x_B)]^{-1} - 2\tilde{\chi} \tag{9}$$

to background-corrected SANS data acquired from matched-pair specimens at 25 °C. The coherent scattered intensity ($I_c(q)$) for a two-component polymer blend, in absolute units of cm^{-1}, is described by

$$I_c(q) = v^{-1}(b_A - b_B)^2 S(q) \tag{10}$$

where b_A and b_B are the coherent scattering lengths of A and B segments, respectively.

$I_c(q)$ data were modeled with eqs 7−10 using a nonlinear least-squares fitting technique, with the degree of polymerization (N) and the statistical segment length (b) as adjustable parameters. Due to the reduced level of deuterium labeling and modest molecular weights, these matched pair mixtures lie far from the critical point for phase separation. As a consequence, $S(q)$ is relatively insensitive to minor variations in χ around the anticipated value.[56] In these calculations, we have simply fixed χ at 1×10^{-4}, approximately the expected isotopic value for these samples.[50,56] The data were fit over the range $0.09 < q < 0.45$ nm^{-1}, and the results are illustrated in Figure 3. Corresponding statistical segment lengths, based on a four-carbon repeat unit at 25 °C, are listed in Table 2. Reported errors are estimated on the basis of the consideration of systematic errors arising from uncertainty in the density measurements necessary to calculate coherent scattering lengths, in absolute calibration,[49] and in background corrections.

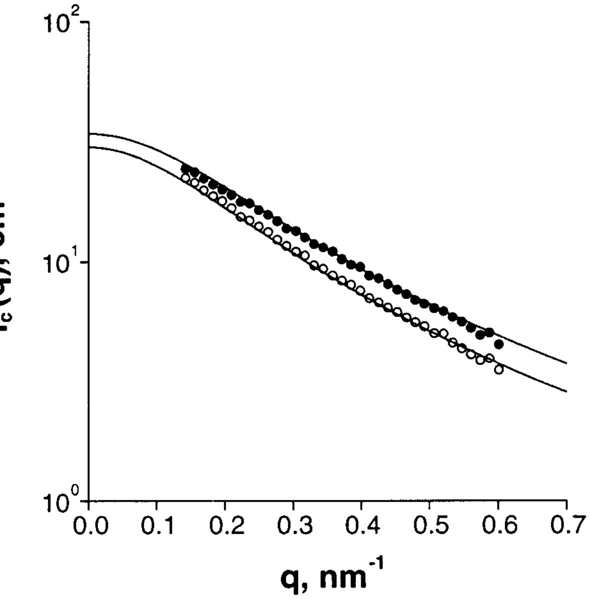

Figure 4. Background-corrected SANS results from d$_6$PEE90/PP3045 blends, with $\phi_{PP3045} = 0.124$ (open symbols) and 0.173 (filled symbols). Solid curves represent a simultaneous best fit of both data sets using eqs 7−14, with the number-average degree of polymerization N_n and the isotactic polypropylene statistical segment length *b* as adjustable parameters. Values of $b = (5.6 \pm 0.2)$ Å and $N_n = 525 \pm 70$ were obtained from this fit, assuming $N_w/N_n = 2.4$.

i-PP Degree of Polymerization and Statistical Segment Length. We have developed a new method for determination of the number-average degree of polymerization (N_n) and the statistical segment length (b) of PP3045, which was necessitated by a lack of deuterated i-PP. On the basis of results discussed below which demonstrate that PEE90 and PP3045 are melt miscible, we prepared the d$_6$PEE90 sample for use as a "polymeric solvent" for PP3045. Low concentrations of i-PP and the relatively low molecular weight of d$_6$PEE90 ensured that our blends of these materials were far from the critical point, minimizing the effect of χ on RPA fits to the data. The high deuterium content of d$_6$PEE90 afforded sufficient contrast to make these measurements feasible.

SANS patterns for $\phi_{PP3045} = 0.124$ and $\phi_{PP3045} = 0.173$ samples at 180 °C, corrected for incoherent background scattering, are shown in Figure 4. In order to fit these data using the RPA, we must account for the polydispersity of the commercial PP3045 component. To do so, we have followed the treatment described by Higgins and Benoit,[57] making the assumption that the molecular weight distribution of the PP3045 sample may be described by the Schultz−Zimm distribution function, expressed in terms of the dimensionless degree of polymerization $u \equiv N/\langle N \rangle$,[58,59]

$$w(u)\,\mathrm{d}u = \frac{k^k}{\Gamma(k)} u^{k-1} \exp(-ku)\,\mathrm{d}u \tag{11}$$

where $\Gamma(k)$ is the gamma function. k, the width of the distribution, is related to the number-average and weight-average degrees of polymerization (N_n and N_w) through

$$\frac{\langle N^2 \rangle^{1/2}}{\langle N \rangle} = \frac{N_w}{N_n} = 1 + \frac{1}{k} \tag{12}$$

Given this molecular weight distribution, it can be shown[57] that the Debye function for polydisperse coils, which we shall refer to as $g_P(x)$, can be expressed as

$$g_P(x_n) = \frac{2}{{x_n}^2}\left[x_n - 1 + \left(1 + \frac{x_n}{k}\right)^{-k}\right] \qquad (13)$$

with

$$x_n = q^2 {R_{g,n}}^2 \qquad (14)$$

where $R_{g,n}$ is the *number-average* radius of gyration. Briber et al.[60] have used a similar approach for the analysis of SANS data for dilute blends of d-polystyrene with a polydisperse sample of poly(vinyl methyl ether).

Using eqs 7–14, the two data sets were simultaneously fit over the range 0.14 nm^{-1} < q < 0.60 nm^{-1}, allowing $N_{n,PP3045}$ and b_{PP3045} to vary. The statistical segment volume, which fixes N, was defined by following our previous convention,[31]

$$v = (1.084 \times 10^{-22}) \exp[6.85 \times 10^{-4}(T - 296)] \qquad (15)$$

with v in cm^3 and T in absolute temperature. This expression corresponds closely to a four-carbon polyolefin repeat unit in the melt state and gives a segment volume of 119.6 Å^3 at 180 °C. $N_{w,PEE90}$ was fixed as 176 (see above), while b_{PEE90} was fixed at 5.3 Å (see below). The Debye function for monodisperse coils (eq 7) was used for the d$_6$PEE90 component. On the basis of the manufacturer's suggestion, we used $(N_w/N_n) = 2.4$ for PP3045, giving a value of $k \approx 0.71$. The value of χ was fixed as 5×10^{-4}, roughly the expected isotopic value.[50,56] Calculations show, however, that variation of χ from 0 to 5×10^{-3} has a negligible effect on the values returned by the fit. From the simultaneous fit to the corrected data shown in Figure 4, and consideration of systematic errors, we find that $N_{n,PP3045} = 525 \pm 70$ and that $b_{PP3045} = 5.6 \pm 0.2$ Å at 180 °C, based on the four-carbon segment volume defined by eq 15.

i-PP/PEE*xx* Phase Behavior. Background-corrected SANS results for $\phi_{PEExxd} = 0.5$ PEE73d/PP3045 and PEE90Ad/PP3045 blends are shown in Figure 5. In order to quantitatively fit these scattering data to the RPA theory, it was necessary to make assumptions concerning the change in the statistical segment length of the PEE*xx* polymers with temperature, as the PEE*xx* matched pair specimens were not studied at 180 °C. We have assumed a linear interpolation between the reported values[61,62] of $(\partial \ln R_g/\partial T)_{PE} = -0.58 \times 10^{-3}$ K^{-1} and $(\partial \ln R_g/\partial T)_{PEE} = 0.2 \times 10^{-3}$ K^{-1} to estimate the high-temperature values listed in Table 2. The Debye functions extracted from the data shown in Figures 3 and 4 were used with these minor temperature corrections. This allowed us to fit the data for the single-phase mixtures using eqs 7–14, with χ as the only adjustable parameter. Results of these fits, over the range 0.09 < q < 0.45 nm^{-1}, are shown in Figure 5 for the PEE73d/PP3045 and PEE90Ad/PP3045 blends; the best-fit values for $\tilde{\chi}$ are $(3.4 \pm 1.5) \times 10^{-4}$ and $(1.9 \pm 2.5) \times 10^{-4}$, respectively. We note that for these samples,[50,56] the expected isotopic contribution to χ is $\approx 0.7 \times 10^{-4}$. Within the uncertainties in g_D, g_P, and the SANS intensity calibration, the RPA calculation quantitatively models the data, leading us to conclude that both systems form nearly ideal single-phase mixtures.

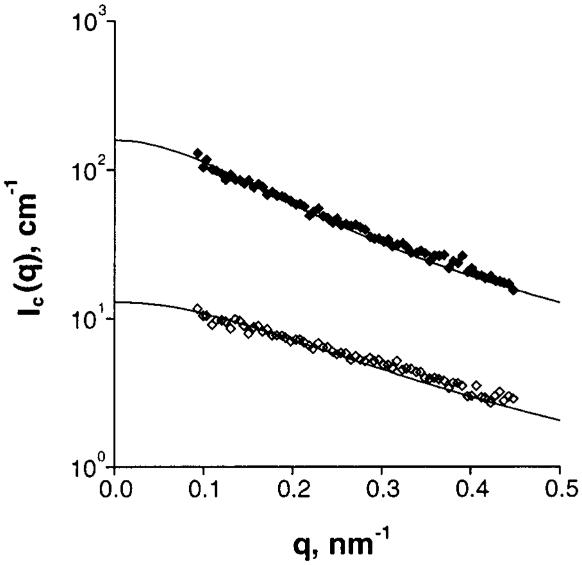

Figure 5. Background-corrected SANS results for PEE73d / PP3045 (filled symbols) and PEE90Ad/PP3045 (open symbols) blends. The PEE73d/PP3045 data have been offset by a factor of 10. The solid curves correspond to best fits using eqs 7–14, with χ as the only adjustable parameter. Values of $\chi_{PEE73d/PP3045} = (3.4 \pm 1.5) \times 10^{-4}$ and $\chi_{PEE90d/PP3045} = (1.9 \pm 2.5) \times 10^{-4}$ were obtained from these fits.

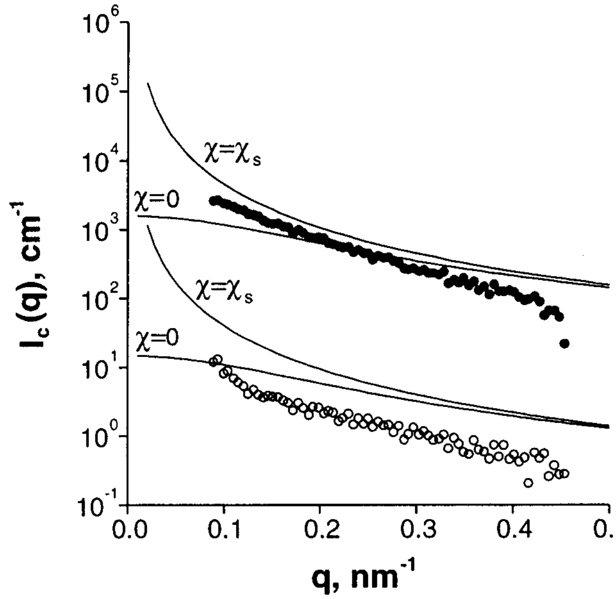

Figure 6. Background-corrected SANS results for PEE46d/PP3045 (open symbols) and PEE62d/PP3045 (filled symbols) blends. The PEE62d/PP3045 data have been offset by a factor of 100. In each case, the solid lines have been calculated for the limits of ideal mixing ($\chi = 0$) and thermodynamic stability ($\chi = \chi_s$).

In Figure 6, the measured background corrected scattering patterns for the PEE46d/PP3045 and PEE62d/PP3045 blends at 180 °C are compared to calculations made using eqs 7–14 for the limiting cases of $\chi = 0$ (ideal mixing) and $\chi = \chi_s$ (thermodynamic stability). The experimental data for the PEE46d/PP3045 mixture falls outside the window of possible scattering patterns for single-phase blends over the entire q range, indicating immiscibility. This finding is consistent with those of Alamo et al.,[63] who recently calculated that the scattering at high q from a two-phase polymer melt will always be less than that of a homogeneous melt of the same composition. For two-phase samples, we note that when domain dimensions are large, the "Guinier" regime of the scattering pattern is close to the transmitted beam and is beyond the resolution of traditional pinhole SANS cameras. However, as shown by Alamo et al.[63] and Bates et al.,[64] the scattering cross section generally contains a strong component of "Porod" scattering from the domain interfaces ($I(q) \sim q^4$) in the q range 0.01−0.1 nm^{-1}. At higher q values, $0.1\ \text{nm}^{-1} < q < 1\ \text{nm}^{-1}$, the "Debye" regime is observed, in which lower intensity scattering arises from molecules within the domains, with $I(q) \sim q^2$. The low-q cutoff of these data at 0.09 nm^{-1} prevents us from unambiguously observing the Porod regime for the PEE46d/PP3045 sample. However, the high-q scattering behavior of this sample, with a coherent scattering intensity 1 order of magnitude less than that of the PEE90 and PEE73 blends, clearly identifies it as phase separated.

Likewise, the comparison of the PEE62d/PP3045 scattering data to the $\chi = 0$ and $\chi = \chi_s$ cases (also shown in Figure 6) indicates that this mixture has also phase separated, as the single-phase RPA fails to fit the scattering data at high q. However, these data fall closer to the single-phase window than the data for the PEE46d/PP3045 blend. We note that setting $\chi < 0$ does not improve agreement between the calculated and measured results for these two samples. Taken together, the results shown in Figures 5 and 6 identify a "window" in EE content where the PEE*xx* polymers are miscible with i-PP, when both blend components are of $M_w \approx 70\,000$. On the low end, the limit is between 62 and 73% EE segments, while on the high end, the limit is higher than 90%.

These conclusions are supported by the optical characteristics of the blends. Visual inspection of the samples at room temperature revealed complete opacity in PEE46d/PP3045 and some degree of opalescence in PEE62d/PP3045. Since the i-PP component in all the blends is partially crystalline at room temperature, we cannot make quantitative statements about melt state phase behavior on this basis alone. Nevertheless, these observations are consistent with crystallization from a macroscopically phase-separated state. In contrast, the PEE73d/PP3045 and PEE90Ad/PP3045 specimens were markedly more translucent at room temperature.

4. Discussion

The primary purpose of this study was to determine whether the apparent melt dispersibility of PEE73-containing diblock copolymers in i-PP[8] would translate into true thermodynamic compatibility of i-PP and PEE*xx* random copolymers. Our results establish that saturated, anionically polymerized 1,2/1,4-polybutadienes with roughly 73% to 90% ethylethylene repeat units can form nearly ideal single-phase melt mixtures with i-PP.

Along with the obvious practical implications of this work, our findings contribute to a general, evolving understanding of polyolefin thermodynamics. Here we restrict our attention to the theoretical and experimental treatments outlined in the Introduction. Evaluation of our "miscibility window" using the solubility parameter approach[17−25] is not possible without quantitative knowledge of $\delta(T)$.[65] However, our statistical segment length measurements for the PEE*xx* materials are consistent with those reported by Graessley et al.[24,66] Taking $\delta_{\text{PEE97}} = 0$ as a reference,[24,67] the magnitude of our reported χ parameters for PEE73/PP3045 and PEE90/PP3045 are consistent with $\delta_{\text{i-PP}} \approx 0.31\ \text{MPa}^{1/2}$ at 180 °C. This is close to the value of 0.25 MPa$^{1/2}$ that Graessley et al.[24] have reported for an atactic polypropylene (prepared by hydrogenation of poly(2-methylpentadiene)) at 167 °C. We note that on a four-carbon repeat unit basis, $b_{\text{a-PP}} = 6.0$ Å.[62] This suggests that the miscibility of i-PP and a-PP observed by Lohse[6] is qualitatively consistent with both the solubility parameter approach and the conformational asymmetry theory.

Since our initial identification of an apparent correlation between statistical segment length differences and miscibility in polyolefins,[31] we have pursued theory[28−30] and experiments[8,9] that might aid in designing commercially useful blends. The concept of an excess entropy of mixing, driven by conformational asymmetry,[31] guided our preparation of the PEE*xx* polymers. Our newly determined i-PP statistical segment length yields $\beta_{\text{i-PP}}{}^2 = 4.36 \times 10^{-2}$ Å^{-1} at 180 °C. This is nearly symmetrically placed between the values of β^2 for PEE73 and PEE90. ($\beta_{\text{PEE73}}{}^2 = 5.18 \times 10^{-2}$ Å^{-1}, with $\epsilon_{\text{PEE73/i-PP}} = 1.19$; $\beta_{\text{PEE90}}{}^2 = 3.77 \times 10^{-2}$ Å^{-1}, with $\epsilon_{\text{i-PP/PEE90}} = 0.83$.) This finding is in qualitative agreement with the conformational asymmetry theory and with the observed correlation between ϵ and miscibility in polyolefin blends.[24,31]

However, we note that at 180 °C, the limit of single-phase stability occurs between $xx = 62$ and 73 for $N_w \approx 1300$ blends (i.e. $1.19 \le \epsilon \le 1.27$). From this, calculation of $\Lambda_b{}^{-1}$ based on eq 3 yields $2.12 \le \Lambda_b{}^{-1} \le 2.62$ Å. This value is considerably smaller than anticipated for the cutoff length associated with the conformational asymmetry theory.[29,30] Graessley et al.[24] have drawn a similar conclusion from their results, as noted in the Introduction.

Finally, we briefly discuss our new determination of the i-PP statistical segment length. To our knowledge, this important conformational parameter has only been measured once before in the melt state,[68] although several Θ-solvent values have been obtained.[62] Ballard et al.[39] reported $(\langle R_{g,w}{}^{1/2}\rangle^2/M_w)^{1/2} = 0.34$ (Å mol$^{1/2}$)/g$^{1/2}$ based on SANS measurements of a mixture of hydrogenous and perdeuterous i-PP at 200 °C. Using eq 1, and assuming[39] $(\partial \ln R_g/\partial T)_{\text{i-PP}} \approx 0$, this translates into $b_{\text{i-PP},180}$ °C = 5.4 Å on a three-carbon repeat unit basis, or 6.2 Å for a four-carbon statistical segment, about 10% greater than our determination. Although the absolute magnitude of the difference is small, it has a significant impact on how we interpret our results, as discussed in the previous paragraphs. While we cannot be certain of the exact origins of this discrepancy, we point out that isotope effects were not recognized two decades ago, and Ballard et al.[39] acknowledged both sample degradation and uncertainties in background corrections at elevated temperatures.

Acknowledgment. We are grateful to Mark Matsen for his assistance with the analysis of scattering data from mixtures containing polydisperse polymers and Damian Hajduk for helpful discussions. This work was supported by the Center for Interfacial Engineering (CIE), an NSF Engineering Research Center at the University of Minnesota. The research at Oak Ridge was supported by the Division of Materials Sciences, U.S. Department of Energy, under Contract No. DE-AC05-96OR22464 with Lockheed Martin Energy Research Corp.

References and Notes

(1) Plochocki, A. In *Polymer Blends*; Paul, D. R., Newman, S., Eds.; Academic: New York, 1978; Vol. 2, Chapter 21.

(2) Lovinger, A. J.; Williams, M. L. *J. Appl. Polym. Sci.* **1980**, *25*, 1703.

(3) Wignall, G. D.; Child, H. R.; Samuels, R. J. *Polymer* **1982**, *23*, 957.
(4) Coppola, F.; Greco, R.; Martuscelli, E.; Kammer, H. W.; Kummerlowe, C. *Polymer* **1987**, *28*, 47.
(5) D'Orazio, L.; Mancarella, C.; Martuscelli, E.; Sticotti, G.; Massari, P. *Polymer* **1993**, *34*, 3671.
(6) Lohse, D. J. *Polym. Eng. Sci.* **1986**, *26*, 1500.
(7) Bianchi, L.; Cimmino, S.; Forte, A.; Greco, R.; Martuscelli, E.; Riva, F.; Silvestre, C. *J. Mater. Sci.* **1985**, *20*, 895.
(8) Bates, F. S.; Kumar, A.; Schulz, M. F. *J. Polym. Sci. B* **1995**, *33*, 1423.
(9) Kumar, A. M.S. Thesis, University of Minnesota, 1996.
(10) Curro, J. G.; Schweizer, K. S. *Macromolecules* **1990**, *23*, 1402.
(11) Curro, J. G.; Yethiraj, A.; Schweizer, K. S.; McCoy, J. D.; Honnell, K. G. *Macromolecules* **1993**, *26*, 2655.
(12) Schweizer, K. S. *Macromolecules* **1993**, *26*, 6050.
(13) Schweizer, K. S.; Singh, C. *Macromolecules* **1995**, *28*, 2063.
(14) Singh, C.; Schweizer, K. S. *Macromolecules* **1995**, *28*, 8692.
(15) Dudowicz, J.; Freed, K. F. *Macromolecules* **1991**, *24*, 5076.
(16) Dudowicz, J.; Freed, M. S.; Freed, K. F. *Macromolecules* **1991**, *24*, 5096.
(17) Balsara, N. P.; Fetters, L. J.; Hadjichristidis, N.; Lohse, D. J.; Han, C. C.; Graessley, W. W.; Krishnamoorti, R. *Macromolecules* **1992**, *25*, 6137.
(18) Walsh, D. J.; Graessley, W. W.; Datta, S.; Lohse, D. J.; Fetters, L. J. *Macromolecules* **1992**, *25*, 5236.
(19) Graessley, W. W.; Krishnamoorti, R.; Balsara, N. P.; Fetters, L. J.; Lohse, D. J.; Schulz, D. N.; Sissano, J. A. *Macromolecules* **1993**, *26*, 1137.
(20) Krishnamoorti, R.; Graessley, W. W.; Balsara, N. P.; Lohse, D. J. *J. Chem. Phys.* **1994**, *100*, 3894.
(21) Graessley, W. W.; Krishnamoorti, R.; Balsara, N. P.; Fetters, L. J.; Lohse, D. J.; Schulz, D. N.; Sissano, J. A. *Macromolecules* **1994,** *27*, 2574.
(22) Krishnamoorti, R.; Graessley, W. W.; Balsara, N. P.; Lohse, D. J. *Macromolecules* **1994**, *27*, 3073.
(23) Graessley, W. W.; Krishnamoorti, R.; Balsara, N. P.; Butera, R. J.; Fetters, L. J.; Lohse, D. J.; Schulz, D. N.; Sissano, J. A. *Macromolecules* **1994**, *27*, 3896.
(24) Graessley, W. W.; Krishnamoorti, R.; Reichart, G. C.; Balsara, N. P.; Fetters, L. J.; Lohse, D. J. *Macromolecules* **1995**, *28*, 1260.
(25) Krishnamoorti, R.; Graessley, W. W.; Dee, G. T.; Walsh, D. J.; Fetters, L. J.; Lohse, D. J. *Macromolecules* **1996**, *29*, 367.
(26) Rhee, J.; Crist, B. *Polym. Mater. Sci. Eng.* **1992**, *67*, 209.
(27) Budkowski, A.; Klein, J.; Eiser, E.; Steiner, U.; Fetters, L. J. *Macromolecules* **1993**, *26*, 3858.
(28) Liu, A. J.; Fredrickson, G. H. *Macromolecules* **1992**, *25*, 5551.
(29) Bates, F. S.; Fredrickson, G. H. *Macromolecules* **1994**, *27*, 1065.
(30) Fredrickson, G. H.; Liu, A. J.; Bates, F. S. *Macromolecules* **1994**, *27*, 2503.
(31) Bates, F. S.; Schulz, M. F.; Rosedale, J. H.; Almdal, K. *Macromolecules* **1992**, *25*, 5547.
(32) Helfand, E.; Sapse, A. M. *J. Chem. Phys.* **1975**, *62*, 1327.
(33) In previous publications, we have referred to poly(1-butene) as poly(ethylethylene) (PEE). In this section of the paper, we are faithful to the literature concerning i-PP/i-P1B blends, in which the poly(1-butene) notation has traditionally been used.
(34) Piloz, A.; Decroix, J-Y.; May, J-F. *Angew. Makromol. Chem.* **1976**, *54*, 77.
(35) Canetti, M.; Bonfatti, A. M.; Sadocco, P.; Seves, A.; Pracella, M. *Polym. Networks Blends* **1993**, *3*, 83.
(36) Gohil, R. M.; Petermann, J. *J. Macromol. Sci., Phys.* **1980**, *B18*, 217.
(37) Cham, P. M.; Lee, T. H.; Marand, H. *Macromolecules* **1994**, *27*, 4263.
(38) Bartczak, Z.; Galeski, A.; Pracella, M. L. *J. Appl. Polym. Sci.* **1994**, *54*, 1513.
(39) Ballard, D. G. H.; Cheshire, P.; Longman, G. W.; Schelten, J. *Polymer* **1978**, *19*, 379.
(40) Hillmyer, M. A.; Bates, F. S. *Macromolecules* **1996**, *29*, 6994.
(41) Gilman, H.; Cartledge, F. K. *J. Organomet. Chem.* **1964**, *2*, 447.
(42) Ndoni, S.; Papadakis, C. M.; Bates, F. S.; Almdal, K. *Rev. Sci. Instrum.* **1995**, *66*, 1090.
(43) Young, R. N.; Quirk, R. P.; Fetters, L. J. *Adv. Polym. Sci.* **1984**, *56*, 1.
(44) Tanaka, Y.; Takeuchi, Y.; Kobayashi, M.; Tadokoro, H. *J. Polym. Sci., Polym. Phys. Ed. A-2* **1971**, *9*, 43.
(45) Gehlsen, M. D. Ph.D. Thesis, University of Minnesota, 1994.
(46) These poly(ethylene/ethylethylene) random copolymers may also be described in terms of the number of ethyl branches per 100 backbone carbons. Using our "PEE*xx*" notation, the number of ethyl branches per 100 backbone carbons may be calculated as $(50xx/[200 - xx])$. As an example, PEE46 has 15 ethyl branches per 100 backbone carbons.
(47) Van Krevelen, D. W. *Properties of Polymers*; Elsevier: Amsterdam, 1994.
(48) On the basis of the SANS results, discussed in the Results and Analysis section, we have found a value of $N_{\mathrm{w,PP3045}} \approx 1260$. This value for the degree of polymerization of PP3045 is about 45% less than that suggested by the manufacturer. Recent high-temperature SEC results in our laboratory suggest that i-PP degrades upon heating to temperatures ≥ 200 °C, even in inert atmosphere or under vacuum. However, within error, we observed identical SANS structure factors for two sets of PP3045-containing miscible blends that were prepared using different techniques and measured at different neutron sources.
(49) Wignall, G. D.; Bates, F. S. *J. Appl. Crystallogr.* **1988**, *20*, 28.
(50) Bates, F. S.; Fetters, L. J.; Wignall, G. D. *Macromolecules* **1988**, *21*, 1086.
(51) For a further discussion of this effect, see Figure 1 and the accompanying text in ref 49.
(52) Balsara, N. P.; Lohse, D. J.; Graessley, W. W.; Krishnamoorti, R. *J. Chem. Phys.* **1994**, *100*, 3905.
(53) Reichart, G. C.; Register, R. A.; Graessley, W. W.; Krishnamoorti, R.; Lohse, D. J. *Macromolecules* **1995**, *28*, 8862.
(54) Debye, P. *J. Phys. Colloid Chem.* **1947**, *51*, 18.
(55) de Gennes, P-G. *Scaling Concepts in Polymer Physics*; Cornell University Press: Ithaca, NY, 1979.
(56) Gehlsen, M. D.; Rosedale, J. H.; Bates, F. S.; Wignall, G. D.; Hansen, L.; Almdal, K. *Phys. Rev. Lett.* **1992**, *68*, 2452.
(57) Higgins, J.; Benoit, H. *Polymers and Neutron Scattering*; Oxford University Press: Oxford, U.K., 1994.
(58) Schultz, G. V. *Z. Phys. Chem. Abt.* **1939**, *B43*, 25.
(59) Zimm, B. H. *J. Chem. Phys.* **1948**, *16*, 1099.
(60) Briber, R. M.; Bauer, B. J.; Hammouda, B. *J. Chem. Phys.* **1994**, *101*, 2592.
(61) Boothroyd, A. T.; Rennie, A. R.; Boothroyd, C. B. *Europhys. Lett.* **1991**, *15*, 715.
(62) Zirkel, A.; Urban, V.; Richter, D.; Fetters, L. J.; Huang, J. S.; Kampmann, R.; Hadjichristidis, N. *Macromolecules* **1992**, *25*, 6148.
(63) Alamo, R. G.; Graessley, W. W.; Krishnamoorti, R.; Lohse, D. J.; Londono, J. D.; Mandelkern, L.; Stehling, F. C.; Wignall, G. D. *Macromolecules* **1997**, *30*, 561.
(64) Bates, F. S.; Dierker, S. B.; Wignall, G. D. *Macromolecules* **1986**, *19*, 1938.
(65) Walsh et al.[18] have reported the critical properties of i-PP derived from fitting two different equations-of-state to *PVT* data. Although α_{P} and β_{T} can be extracted from these results, the uncertainties associated with the reduced functions exceeds the required sensitivity in $\delta_{\mathrm{i-PP},PVT}$.
(66) We have used a slightly different notation than Graessley and co-workers.[17] They would refer to our "PEE*xx*h" materials as "Hxx", and our "PEE*xx*d" materials as "Dxx".
(67) This definition is consistent with that of Graessley et al.,[24] who define $\delta_{\mathrm{H97}} = 0$ as a reference at all temperatures.
(68) Lohse[6] has published a SANS measurement of $R_{\mathrm{g},z}$ and M_{w} for an isotopic i-PP blend in the melt. However, he did not report (N_z/N_{w}), without which we cannot directly compare his result to ours.

MA961383H